Available online at www.sciencedirect.com
SCIENCE DIRECT
Chemical Physics 321 (2006) 159–170
Chemical Physics
www.elsevier.com/locate/chemphys

VUV absorption spectrum of acetic acid between 6 and 20 eV

Sydney Leach [a,*], Martin Schwell [b], Sun Un [c], Hans-Werner Jochims [d], Helmut Baumgärtel [d]

[a] LERMA, CNRS-UMR 8112, Observatoire de Paris-Meudon, 5 place Jules-Janssen, 92195 – Meudon, France
[b] Laboratoire Interuniversitaire des Systèmes Atmosphériques (LISA), CNRS-UMR 7583, Universités Paris 7 et 12, 61 Avenue du Général de Gaulle, 94010 Créteil, France
[c] Service de Bioénergetique, CNRS URA 2096, DBJC, CEA Saclay, 91191 Gif-sur-Yvette, France
[d] Institut für Physikalische und Theoretische Chemie der Freien Universität Berlin, Takustr. 3, 14195 Berlin, FR Germany

Received 10 June 2005; accepted 18 August 2005
Available online 11 October 2005

Abstract

Absorption spectra of acetic acid were measured between 6 and 20 eV at a resolution of 8 meV. Previous measurements had a spectral limit of 11.7 eV. Analysis and band assignment were aided by data from theoretical calculations on valence states and from photoelectron spectroscopy. Valence transitions and $n$sa′ ← 13a′, $n$pa′ ← 13a′ and $n$da′ ← 13a′ Rydberg transitions converging to the ground state of CH_3COOH^+, as well as transitions converging to the first excited state of the ion are discussed and assigned in the spectral region below 12 eV. Our assignments of valence transitions differ in many aspects from those of previous studies. Most of the Rydberg bands have never previously been assigned. Observation, analysis and possible assignments of absorption features between 12 and 20 eV were carried out for the first time. Rydberg bands converging to the higher ionization limits merge to form broad absorption features. Some absorption features in the 14–17 eV region are assigned to two types of valence σ*(C–H) ← σ transitions.

Keywords: Acetic acid; VUV absorbption spectra; Electronic transition calculations and assignments

1. Introduction

Acetic acid, CH_3COOH, is considered to be an important trace species in the Earth's atmosphere [1]. It is also one of the possible building blocks of biomolecules [2] and it is formed in Miller–Urey experiments on simulated atmospheres of the Early Earth [3]. It has been observed by radioastronomy in the SGR B2 Large Molecule Heimat (LMH) source, using interferometric arrays [4]. There is reason to believe that the amino acid glycine could also exist in an interstellar source of CH_3COOH [5], and indeed this amino acid has been reported to have been detected in three hot molecular cores, including Sgr B2 (N-LMH), where CH_3COOH is also observed [6]. Although no direct cometary observation of acetic acid has been made, abundance upper limits have been determined for various comets, based on radio spectroscopic observations, in particular a limit of 0.06% for acetic acid in the bright comet Hale–Bopp [7]. Increased sensitivity in new ground-based radiotelescopes, and the possibility of more extended search frequencies in space-borne observatories, make it likely that acetic acid will be observed in future cometary studies. The photophysical properties of CH_3COOH in the UV and VUV are thus of direct interest for undertaking radioastronomy searches, for cometary science and for atmospheric and exobiology studies.

We have carried out a number of photophysical measurements on acetic acid, in particular on dissociative ionization yields over the 6–22 eV energy range, the dispersed fluorescence spectrum excited at several VUV photon energies, and excitation spectra for various fluorescence bands [8]. The present work concerns the absorption spectrum

* Corresponding author. Tel.: +33 1 4507 7561; fax: +33 1 4507 7100.
E-mail address: sydney.leach@obspm.fr (S. Leach).

0301-0104/$ - see front matter © 2005 Elsevier B.V. All rights reserved.
doi:10.1016/j.chemphys.2005.08.044

of CH_3COOH between 6 and 20 eV. The absorption results have been important for interpretation of the results of the photophysical investigations. Earlier absorption and fluorescence spectra with comparable resolution were limited to measurements below 11.7 eV [9,10]. Reported electron energy loss spectra [11] of CH_3COOH, limited to about 15 eV, are of low resolution.

The earlier absorption spectra reported by Bell et al. [9] are in the 4.8–11.27 eV and by Suto et al. [10] in the 5.17–11.7 eV region. Barnes and Simpson [12] studied the 5.0–9.9 eV and Nagakura et al. [13] the 6.5–8.0 eV region absorption. Absolute absorption cross-section values of Suto et al. are lower than those measured by Barnes and Simpson and by Nagakura et al. Since absorption cross-sections at $\lambda > 190$ nm are very small it was necessary for them to use higher gas pressures (up to 0.7 Torr); thus acetic acid dimers could have contributed to measured absorption cross-sections in this spectral region, a region which we did not explore. The excited states of CH_3COOH were labelled A, A′, B, C, etc. by Bell et al. [9] by analogy with HCOOH. They suggested that absorption bands at $\lambda < 155$ nm are probably Rydberg series converging on the ground state of the acetic acid ion, but made few assignments.

2. Experimental

Absorption spectra were measured with an experimental set-up whose essential components and procedure have been described previously [14] so that only a brief resumé is given here. Monochromatised synchrotron radiation was obtained from the Berlin electron storage ring BESSY I (multi-bunch mode) in association with a M-225 McPherson monochromator modified to have a focal length of 1.5 m, and a gold coated spherical diffraction grating having 1200 lines/mm. Spectral dispersion was 5.6 Å/mm. The mean geometric slit width was 0.1 mm. The 30 cm long absorption cell is separated from the monochromator vacuum by a 1 mm thick stainless steel microchannel plate (MCP). Acetic acid gas pressures were in the range 20–40 μbar, measured with a Balzers capacitance manometer. This is a pressure region where the concentration of acetic acid dimers to monomers is negligibly small [10]. The small pressure gradient inside the absorption cell, due to the gas leak through the MCP, does not significantly affect the optical density measurements. The use of the MCP enables us to know the precise optical pathlength, the pressure drop being by a factor of the order of 1000, which ensures linearity in the Beer–Lambert analysis of the optical density measurements. VUV light transmission efficiency of the MCP is estimated to be about 10% and the transmitted light was largely sufficient for absorption measurements. Transmitted radiation strikes a window covered with a layer of sodium salicylate whose ensuing fluorescence was detected by a photomultiplier. We remark that the use of a laminar-type grating results in a very low (only few percent) contribution to second order radiation in the 10–20 eV region. Second order effects will be also very low below 10 eV because the gas column in the absorption cell reduces high energy radiation transmission much more than the low energy part. The determination of absolute absorption cross-sections, using the Beer–Lambert law, provided cross-section values whose uncertainties were ±10%.

Two scans, one with and one without acetic acid gas were carried out for determining the absorption spectrum. During a scan, the VUV light intensity falls off slightly due to continuous loss of electrons in the storage ring. The incident light intensity is furthermore a function of the energy-dependent reflectance of the diffraction grating. These two factors have been taken into account in normalisation of the spectra, which were recorded at an energy interval of 9 meV.

Absorption measurements were carried out in April 1999 at two gas pressures, 20 and 40 μbar. They were repeated in October 1999. The results were quasi-identical. The resolution is about 8 meV (at 100 nm) and the precision of the energy scale is ±5 meV. Commercial CH_3COOH of highest available purity grade was used, without further purification.

3. Calculations

Quantum chemical calculations were carried out using GAUSSIAN-03 revision B.05 [15]. An initial geometry optimization of acetic acid was performed using the hybrid density functional B3LYP and 6-311++G(3DF,3PD) basis set. "Tight" convergence criteria were used. The optimized geometry was that of the most stable form, of *cis* configuration, the lowest energy isomer. The calculated structural parameters are in good agreement with the gas phase experimental values determined by electron diffraction [16]. The calculated and, in brackets, the gas phase experimental values are as follows (bondlengths in Ångstrom units, bond angles in degrees): C–O 1.360 (1.364), C=O 1.213 (1.214), C–C 1.506 (1.520), O–H 0.972 (0.970), C–H 1.089 (1.102), C–H 1.094 (1.094), O–O 2.253 (2.264), O–C=O 122.20 (122.80), C–C=O 126.10 (126.60), C–C–O 111.70 (110.60, C–O–H 107.00 (107.00). Normal mode analysis confirmed that the final optimized geometry was a true potential energy minimum. The energies and oscillator strengths of transitions to the first 50 electronic excited states were calculated using the time-dependent DFT method [17] with the same hybrid density function and basis set. Such calculations are not expected to provide good values for transition energies beyond about 9 eV in the case of acetic acid, since the eigenvalues are critically dependent on MO energy differences in time-dependent DFT calculations. However, these calculations differentiate well between strong and weak electronic transitions, thus facilitating the valence transition assignments. Molecular orbitals were visualized using the program MOLDEN [18].

4. Results and discussion

4.1. Absorption spectra: general characteristics

The complete absorption spectrum of acetic acid between 6 and 20 eV is given in Fig. 1. Successive sections of the absorption spectra between 6 and 12 eV are shown in Figs. 2 and 3. The band assignments are listed in Table 1 but, for the sake of visual clarity, not all assignments are indicated in the figures. Features measured in the 7–18 eV region are listed as band numbers, energies and band assignments in Table 1, along with the quantum defects of the Rydberg levels, determined for the origin bands of the Rydberg transitions. In Table 1, the energies of the observed features are quoted to 1 meV and to 1 cm^{-1}; the uncertainties in repeated measurements of the peak frequencies of sharp features are of the order of 10–20 cm^{-1} and those of broad features are somewhat greater. The maximum absorption cross-section of 72.2 Mb occurs at 16.83 eV (Fig. 1). Suto et al. [10] published absorption spectra over the 5.17–9.43 eV region, using synchrotron radiation as spectral source. Our cross-sections are in general good agreement with those of Suto et al. in the 6–9.4 eV region common to both measurements and also with the cross-sections of Nagakura et al. [13] who measured the absorption spectrum in the 6.5–8.1 eV region at low resolution.

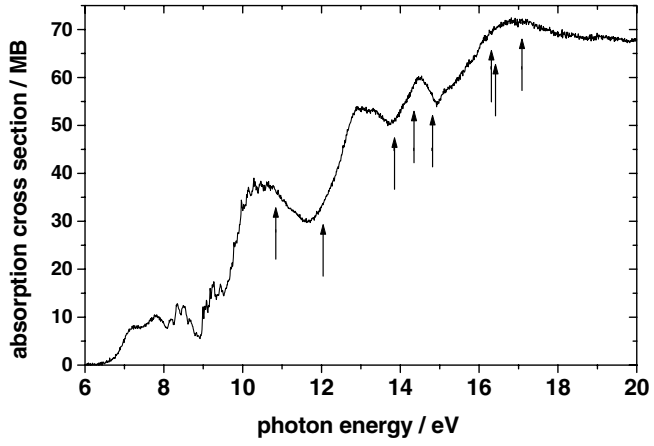

Fig. 1. Overview of the absorption spectrum of CH_3COOH in the 6–20 eV region. Arrows indicate vertical ionization energies.

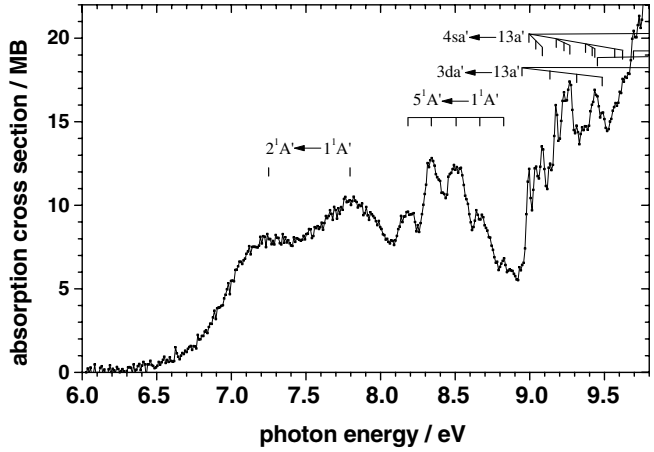

Fig. 2. CH_3COOH absorption spectrum: 6.0–9.8 eV.

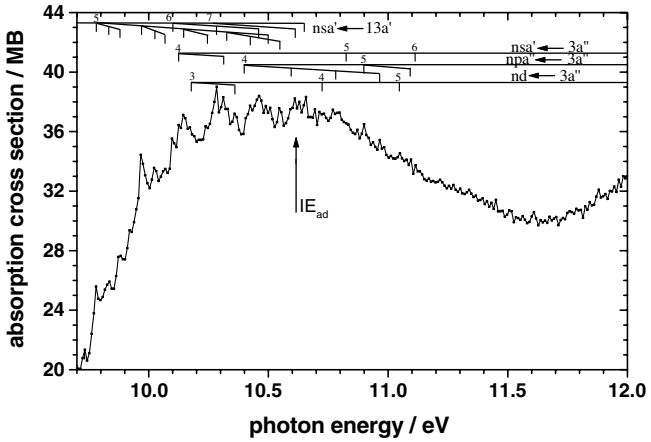

Fig. 3. CH_3COOH absorption spectrum: 9.7–12 eV.

Bell et al. [9] carried out photographic absorption spectroscopy of acetic acid in the 4.8–11.3 eV region. Electron energy loss spectra (EELS) of acetic acid have been measured in the 5–15 eV region [11] and assignments of valence shell and Rydberg transitions have been discussed by comparison with the optical absorption spectra of Barnes and Simpson [12]. A comparison between the published EELS spectrum and our and other optical absorption spectra clearly indicate that the EELS resolution is insufficient for anything but qualitative discussion.

4.2. Absorption spectra: theoretical considerations and implications for analysis

The distinction between valence and Rydberg transitions is not always easy to establish since there can be quite a lot of mixing between valence and Rydberg states. Our analysis of the absorption spectrum of acetic acid seeks to characterise those states that are predominantly valence or predominantly Rydberg in character. For this we use a number of criteria, such as comparison with calculated energies and transition strengths, the nature of the molecular orbitals involved in the optical transitions and their effects on structural and vibrational properties. These criteria will be discussed as they arise in this work.

In order to analyse valence and Rydberg transitions in the absorption spectra of acetic acid, and to distinguish between them, we first examine the electron configurations and structures of CH_3COOH and CH_3COOH^+.

4.2.1. CH_3COOH electron configurations and structures

The ground state of neutral acetic acid formally belongs to the C_s symmetry group. As stated above, its most stable form corresponds to the lowest energy isomer, of

Table 1
Acetic acid absorption features and transition assignments in the 6.8–18 eV spectral region

Band No.	Energy/eV	Frequency ν/cm^{-1}	Assignment	Quantum defect[a] δ
1	7.250	58,479	$2^1A' \leftarrow 1^1A'$	
2	7.795	62,874	See text	
3	8.183	66,004	$5^1A' \leftarrow 1^1A'(0_0^0)$	
4	8.340	67,270	$5^1A' \leftarrow 1^1A'(\nu_{\mathrm{def}\,0}^1)$	
5	8.506	68,609	$5^1A' \leftarrow 1^1A'(\nu_{\mathrm{def}\,0}^2)$	
6	8.665	69,892	$5^1A' \leftarrow 1^1A'(\nu_{\mathrm{def}\,0}^3)$	
7	8.825	71,182	$5^1A' \leftarrow 1^1A'(\nu_{\mathrm{def}\,0}^4)$	
8	8.948	72,170	$3da' \leftarrow 13a'(0_0^0)$	0.14 (3d)
9α	8.994	72,546	$4sa' \leftarrow 13a'(0_0^0)$	1.10 (4s)
10β	9.040	72,917	$4sa' \leftarrow 13a'(12_0^1)$	
11γ	9.084	73,272	$4sa' \leftarrow 13a'(12_0^2)$	
12	9.135	73,683	$3da' \leftarrow 13a'(4_0^1)$	
13α	9.177	74,022	$4sa' \leftarrow 13a'(4_0^1)$	
14β	9.229	74,441	$4sa' \leftarrow 13a'(4_0^112_0^1)$	
15γ	9.268	74,756	$4sa' \leftarrow 13a'(4_0^112_0^2); 3pa'' \leftarrow 3a''(0_0^0)$	*0.60* (3p)
16	9.314	75,127	$3da' \leftarrow 13a'(4_0^2)$	
17α	9.373	75,603	$4sa' \leftarrow 13a'(4_0^2)$	
18β	9.418	75,966	$4sa' \leftarrow 13a'(4_0^212_0^1)$	
19γ	9.435	76,103	$4sa' \leftarrow 13a'(4_0^212_0^2); 4pa' \leftarrow 13a'(0_0^0)$	0.64 (4p)
20	9.453	76,248	$3pa'' \leftarrow 3a''(4_0^1)$	
21	9.485	76,506	$3da' \leftarrow 13a'(4_0^3)$	
22β	9.569	77,184	$4sa' \leftarrow 13a'(4_0^312_0^1)$	
23γ	9.622	77,611	$4sa' \leftarrow 13a'(4_0^312_0^2); 4pa' \leftarrow 13a'(4_0^1)$	
24	9.695	78,200	$4da' \leftarrow 13a'(0_0^0)$	0.15 (4d)
25	9.732	78,498	$7^1A' \leftarrow 1^1A'(0_0^0)$	
26ε	9.781	78,894	$5sa' \leftarrow 13a'(0_0^0); 4pa' \leftarrow 13a'(4_0^2)$	0.96 (5s)
27ζ	9.833	79,313	$5sa' \leftarrow 13a'(12_0^1)$	
28η	9.880	79,692	$5sa' \leftarrow 13a'(12_0^2)$	
29	9.922	80,031	$5pa' \leftarrow 13a'(0_0^0)$	0.57 (5p)
30ε	9.970	80,418	$5sa' \leftarrow 13a'(4_0^1)$	
31ζ	10.026	80,870	$5sa' \leftarrow 13a'(4_0^112_0^1)$	
32η	10.068	81,208	$5sa' \leftarrow 13a'(4_0^112_0^2); 5da' \leftarrow 13a'(0_0^0)$	0.13 (5d)
33	10.101	81,475	$6sa' \leftarrow 13a'(0_0^0); 5pa' \leftarrow 13a'(4_0^1)$	0.86 (6s)
34	10.125	81,663	$4sa' \leftarrow 3a''(0_0^0)$	*0.99* (4s)
35ε	10.146	81,838	$5sa' \leftarrow 13a'(4_0^2); 6sa' \leftarrow 13a'(12_0^1); 6pa' \leftarrow 13a'(0_0^0)$	0.61 (6p)
36	10.178	82,091	$3d \leftarrow 3a''(0_0^0)$	*0.06* (3d)
37η	10.245	82,636	$5sa' \leftarrow 13a'(4_0^212_0^2); 7sa' \leftarrow 13a'(0_0^0)$	0.94 (7s)
38	10.283	82,943	$6sa' \leftarrow 13a'(4_0^1); 5pa' \leftarrow 13a'(4_0^2); 7pa' \leftarrow 13a'(0_0^0)$	0.60 (7p)
39	10.313	83,185	$4sa' \leftarrow 3a''(4_0^1)$	
40 ε	10.326	83,284	$5sa' \leftarrow 13a'(4_0^3); 6sa' \leftarrow 13a'(4_0^112_0^1); 6pa' \leftarrow 13a'(4_0^1)$	
41	10.360	83,564	$3d \leftarrow 3a''(4_0^1)$	
42	10.399	83,873	$4pa'' \leftarrow 3a''(0_0^0)$	*0.67* (4p)
43η	10.424	84,080	$5sa' \leftarrow 13a'(4_0^312_0^2); 7sa' \leftarrow 13a'(4_0^1)$	
44	10.459	84,362	$6sa' \leftarrow 13a'(4_0^2); 7pa' \leftarrow 13a'(4_0^1)$	
45ε	10.499	84,685	$5sa' \leftarrow 13a'(4_0^4); 6pa' \leftarrow 13a'(4_0^2)$	
46ζ	10.548	85,080	$5sa' \leftarrow 13a'(4_0^412_0^1)$	
47	10.595	85,454	$4pa'' \leftarrow 3a''(4_0^1)$	
48	10.612	85,596	$7sa' \leftarrow 13a'(4_0^2)$	
49	10.654	85,935	$7pa' \leftarrow 13a'(4_0^2)$	
50	10.724	86,500	$4d \leftarrow 3a''(0_0^0)$	*0.12* (4d)
51	10.781	86,960	$4pa'' \leftarrow 3a''(4_0^2)$	
52	10.794	87,059	$7sa' \leftarrow 13a'(4_0^3)$	
53	10.825	87,314	$5sa' \leftarrow 3a''(0_0^0)$	*0.89* (5s)
54	10.899	87,911	$5pa'' \leftarrow 3a''(0_0^0)$	*0.68* (5p)
55	10.965	88,444	$4pa'' \leftarrow 3a''(4_0^3)$	
56	11.047	89,105	$5d \leftarrow 3a''(0_0^0)$	*0.17* (5d)
57	11.092	89,463	$5pa'' \leftarrow 3a''(4_0^1)$	
58	11.113	89,632	$6sa' \leftarrow 3a''(0_0^0)$	*0.87* (6s)
59	12.922	104,229	[b]	
60	13.330	107,520	[b]	
61	14.500	116,957	σ^*(C–H) $\leftarrow \sigma$ (non-n.h. transition)[d]	
62	15.125	121,991	[c]	
63	15.770	127,201	[c]	
64	16.830	135,751	σ^*(C–H) $\leftarrow \sigma$[d]	

[a] Quantum defects are of the origin bands of Rydberg series converging to the ion ground state $1^2A'$ and, in italics, of Rydberg levels converging to the first excited ion state $1^2A''$.

[b] Region of broad overlapping Rydberg bands converging to the $2^2A''$ ion state.

[c] Broad overlapping Rydberg bands converging to the highly excited ion states.

[d] See text.

cis configuration, in which both the OH bond and a CH bond are eclipsed with the carbonyl bond. The *trans* form is calculated (ab initio methods [19]) to lie 2100–2500 cm^{-1} above the *cis* configuration.

The electron configuration of CH_3COOH is, according to our molecular orbital energy calculations:

$$\ldots\ldots(7a')^2(8a')^2(9a')^2(10a')^2(1a'')^2(11a')^2(12a')^2(2a'')^2(3a'')^2(13a')^2, \quad 1^1A'.$$

The calculated MO energies, relative to the experimental ionization energy, are compared in Table 2 with reported values of vertical ionization energies determined from He I [20] and He II photoelectron spectroscopy [21] and, for inner shell ionizations, the results of inner shell electron energy loss (ISEEL) spectroscopy [22]. This table also contains the results of HAM/3 [21] and GAUSSIAN-70 [20] calculations of molecular orbital energies, as well as those of Urquhart and Ade [23] for inner shell orbitals. Our calculated order of the occupied molecular orbitals is the same as that in the GAUSSIAN-70, 4-31G calculations of Carnovale et al. [20], but the order of the close-lying 1a″ and 10a′ MO's are reversed in the HAM/3 calculations of von Niessen et al. [21].

Agreement between our calculated valence shell orbital energies and the experimental values is very satisfactory. Our calculated values for the valence MO's are more extensive than the other theoretical values in Table 2, and they agree somewhat better with the results of photoelectron spectroscopy. The inner shell orbitals are in large measure 1s atomic orbitals. Our calculations on the inner shell orbitals, presented here for completion, fall short of the experimental values, no doubt due to core hole effects, which are not adequately dealt with in our calculation method. This is reflected in the non-negligible population of 2s carbon or oxygen atomic orbitals which we find from a population analysis of each of the four deepest molecular orbitals. An improved virtual orbital approximation in calculations using Kosugi's GSF3 package [24], enabled Urquhart and Ade [23] to calculate inner shell values in good agreement with carbonyl core values determined by ISEELS. It is of interest, nevertheless, that in our calculations, although the absolute energies of the inner shell MOs are 20–30 eV below the experimental values, the energy differences between the 3a′ and 4a′ orbitals, 3.38 eV, and 1a′ and 2a′ orbitals, 1.56 eV, are similar to the experimental differences for the carbon (4.0 eV) and oxygen (1.8 eV) orbitals (Table 2).

The bonding characters of the highest four occupied molecular orbitals, 13a′, 3a″, 2a″ and 12*a*′, were determined from our MO contour analyses (Fig. 4). They are consistent, insofar as being either a π or a σ orbital, with the assignments of Carnovale et al. [20] and of Cannington and Ham [25], based in part on ratios of HeI/HeII photoelectron spectral band intensities. For the 12a′ MO, they differ from that of Kimura et al. [26] who considered it to be a π orbital, based on partial sums of vertical ionization energies. However, Carnovale et al. [20] observed that the assignment of 12a′ as a σ orbital agrees equally well with the defined partial sums. The bonding characteristics of the next four occupied MO's, given below, are based on our assessment of the assignments of Carnovale et al. [20], Cannington and Ham [25] and Kimura et al. [26].

–13a′ is mainly non-bonding n_O on the O atom lone pair of the carbonyl group,
–3a″ is $\pi_{C=O}$ mixed with n_{OH}, the latter being mainly localised on the O atom of OH,
–2a″ is π_{OCO},
–12a′ is σ_{CC},
–11a′ is σ_{CO} within the O–C–O framework,
–1a″ is π_{OCO} mixed with n_{OH} and π_{CH3},
–10a′ is σ_{OCO},
–9a′ is σ_{OH}.

Table 2
Calculated and experimental vertical ionization energies of acetic acid

Molecular orbital	Calculated IE/eV Present study (GAUSSIAN-03)	Calculated IE/eV HAM/3 ([21])	Calculated IE/eV (GAUSSIAN-70) ([20]) and GSCF3† ([23])	Experimental IE/eV He I PES ([20])	Experimental IE/eV He II PES [21] and ISEEL spectra* [22]
13a′	(10.84)	10.96	11.16	10.84	10.9
3a″	12.08	11.96	11.79	12.03	12.1
2a″	13.90	13.81	13.82	13.84	(13.6–15.0)
12a′	14.01	13.98	13.94	14.34	(13.6–15.0)
11a′	14.39	14.24	14.12	14.80	(13.6–15.0)
1a″	16.00	15.85	16.05	16.3	16.4
10a′	16.25	15.64	16.71	16.4	16.4
9a′	16.57	16.28	17.15	17.08	17.1
8a′	19.86	19.52			20.3
7a′	23.83	23.62			24.4
6a′	30.91	32.00			
5a′	33.34	33.78			
4a′	269.32				291.6*(CH_3)
3a′	272.70		296.52†		295.6*(C=O)
2a′	512.38		533.29†		538.3*(CO)
1a′	513.94				540.1*(OH)

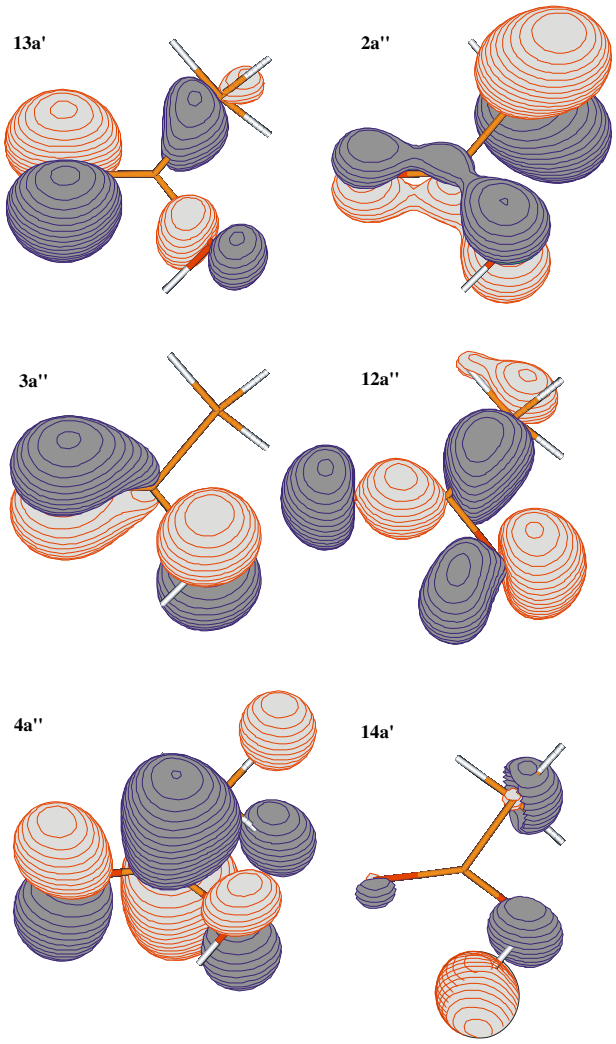

Fig. 4. Acetic acid molecular orbital contours calculated with the Molden programme [18].

Based on analogies with formic acid, we can expect that the lowest unoccupied molecular orbital will be: 4a″, a $\pi^*_{C=O}$ MO. Our initial DFT time-dependent molecular orbital calculations at the 6-31G + (d,f) level with a B2LYP density functional appeared to confirm this, but they predicted that the LUMO + 1, 14a′(σ^*_{OH}) to be only 122 meV higher. This is a relatively small energy difference so that their order could be very sensitive to the type and basis set of the MO calculation. Indeed, further calculations, at the B3LYP + 6-311** level gave the lowest unoccupied molecular orbital as 14a′, with 4a″ lying 147 meV above. Calculations of their molecular orbital contours (Fig. 4) confirmed the bonding properties, mentioned above, of the 14a′ and 4a″ MO's.

The adiabatic ionization energy (IE(ad)) of acetic acid has been reported, by Knowles and Nicholson [29], in an early photoionization mass spectrometry (PIMS) measurement, to be 10.644 ± 0.002 and 10.66 ± 0.01 eV by Villem and Akopyan [30], and by Watanabe et al. [31], from HeI photoelectron spectroscopy, to be 10.664 ± 0.003 eV. In a recent PIMS study of acetic acid [8] we measured IE-(ad) = 10.58 ± 0.02 eV, which is slightly lower than the above values. We consider that the ion ground state $1^2A'$ has the electron configuration: …$(12a')^2(2a'')^2$ $(3a'')^2(13a')$, $1^2A'$. The $1^2A''$ first excited electronic state of the ion is at 11.63 ± 0.01 eV (adiabatic energy from photoelectron spectroscopy [31]), of configuration …$(12a')^2(2a'')^2(3a'')(13a')^2$. The characteristics of higher excited states of the acetic acid ion will be discussed later.

4.2.2. Valence states and transitions of CH_3COOH

Previous assignments of the valence bands in the absorption spectra of acetic acid have been based on correlations between spectra of formic acid and other carboxylic acids [12,27,28]. In line with our previous study on formic acid, we will be concerned with the valence transitions discussed below (Table 3). Considering the effective symmetry of acetic acid to be C_s, we discuss the transition dipoles as being in plane (1A′ ← 1A′), expected to be strong, or out of plane (1A″ ← 1A′), expected to be weak [27,32]:

1) The lowest energy singlet–singlet valence transition, because of its weak intensity (see below), we interpret, on a one electron transition basis, as

$$\ldots(12a')^2(2a'')^2(3a'')^2(13a')^2, \quad 1^1A'$$
$$\rightarrow \ldots(12a')^2(2a'')^2(3a'')^2(13a')(4a''), \quad 1^1A''.$$

Table 3
Valence transitions in acetic acid: calculated and experimental transition energies and oscillator strengths

Transitions between electronic states	Principal configurations involved in electronic transitions[a]	Calculated transition energy (eV) and oscillator strength	Experimental transition energy (eV) and oscillator strength
$1^1A'' \leftarrow 1^1A'$	4a″ ← 13a′; *5a″ ← 13a′*	5.825 (0.0005)	≈6.0 (0.001)
$2^1A' \leftarrow 1^1A'$	14a′ ← 13a′	6.669 (0.0466)	7.25 (0.02)
$3^1A' \leftarrow 1^1A'$	*4a″ ← 3a″*; 15a′ ← 13a′	7.3782 (0.001)	[see text]
$2^1A'' \leftarrow 1^1A'$	14a′ ← 3a″	7.7851 (0.0022)	[see text]
$3^1A'' \leftarrow 1^1A'$	*4a″ ← 13a′*; 5a″ ← 13a′	8.0581 (0.0003)	[see text]
$4^1A' \leftarrow 1^1A'$	16a′ ← 13a′	8.1326 (0.0037)	[see text]
$5^1A' \leftarrow 1^1A'$	*4a″ ← 2a″*; *4a″ ← 3a″*; *5a″ ← 3a″*; *15a′ ← 13a′*	8.4283 (0.1492)	8.18–8.82 (0.045) [see text]
$6^1A' \leftarrow 1^1A'$	17a′ ← 13a′	8.4867 (0.0039)	[see text]
$4^1A'' \leftarrow 1^1A'$	*14a′ ← 3a″*; 15a′ ← 3a″	8.5397 (0.0002)	[see text]
$7^1A' \leftarrow 1^1A'$	18a′ ← 13a′	9.0417 (0.051)	[see text]

[a] Minor components in italics.

This corresponds to a $4a'' \leftarrow 13a'$, $\pi^* \leftarrow n_O$ transition, i.e. promotion of a non-bonding electron on the carbonyl oxygen to an antibonding molecular orbital in the carbonyl carbon. The effect is to modify the molecular geometry from quasi-planar to pyramidal. This weak, out-of-plane, transition, occurs in the 6.0 eV region [28], outside our spectral observation range. It has also been observed in EELS experiments [11]. From the published spectrum of Barnes and Simpson [12] on this broad, almost featureless absorption band, we estimate $f \approx 0.0004$, using the formula $f \approx 9.7 \times 10^{-3} \times \sigma_{max} \times \Delta E_{1/2}$, where the peak absorption cross-section σ_{max} is in Mb, and $\Delta E_{1/2}$ is the FWHM, in eV of an assumed Gaussian band profile [32]. Our calculations agree with these results since they give 5.825 eV as the energy of this transition, mainly resulting from $4a'' \leftarrow 13a'$ and $5a'' \leftarrow 13a'$ molecular orbital excitations, and an oscillator strength of 0.0005 (Table 3). The spectral properties of the observed transition are consistent with the LUMO being 4a″, since if it were the $14a'(\sigma^*_{OH})$ MO the resulting in plane dipole transition would be expected to be much more intense [32]. Indeed, for this transition, our DFT calculation gives an oscillator strength $f = 0.047$ (Table 3).

2) The second valence transition $14a' \leftarrow 13a'$, $2^1A' \leftarrow 1^1A'$, is in-plane (Table 3) . This is the $\tilde{A}'$–X transition in the Bell et al. nomenclature [9]. We observe its peak absorption at 7.25 eV (Fig. 2), in good agreement with previous workers [9–13]. Our estimate of the oscillator strength of this transition is $f \approx 0.020$. This is similar to the analogous in-plane transition band at 7.5 eV in formic acid, whose $f \approx 0.025$ [32]. Our calculations give a transition energy of 6.669 eV, the main MO excitation being $14a' \leftarrow 13a'$, and an oscillator strength of 0.047, as mentioned above. We note that this 7.25 eV band was tentatively assigned by Barnes and Simpson as a $\pi^* \leftarrow n'_O$ transition [12] whereas Robin considers that it corresponds to a $3s \leftarrow n_O$ Rydberg transition [28]. Our valence transition assignment is equivalent to a $\sigma^*_{OH} \leftarrow n'_O$ transition. The $3sa' \leftarrow 13a'$ Rydberg transition could also be part of this band (see later).

3) The next three transitions, in-plane $3^1A' \leftarrow 1^1A'$, and out-of-plane $2^1A'' \leftarrow 1^1A'$ and $3^1A'' \leftarrow 1^1A'$, (Table 3), are calculated to be very weak and are probably part of the broad band whose maximum intensity is at 7.795 eV (Fig. 2). This is another spectral region where one could expect the $3sa' \leftarrow 13a'$ Rydberg transition to occur (see later). We estimate the oscillator strength associated with the 7.795 eV band to be $f \approx 0.03$. This is an order of magnitude greater than the three valence transitions predicted to occur in this spectral region but compatible with a Rydberg transition [28]. Thus it is reasonable to consider that the broad band at 7.795 eV also contains a Rydberg transition (see later). We note that the EELS 7.8 eV peak has been assigned to a $\pi^* \leftarrow \pi$ transition [11], whereas Barnes and Simpson [12], assigned the 7.795 eV band as the $3s(\sigma^*) \leftarrow n_O$ in-plane transition.

4) Several valence transitions are calculated to occur in the 8–9 eV spectral region (Table 3), only one of which, $5^1A' \leftarrow 1^1A'$ is predicted to be a strong transition. This is observed as a series of broad bands, at 8.183, 8.340, 8.506, 8.665 and 8.825 eV (Fig. 2), in good agreement with the observations of Bell et al. [9] who called this the C–X transition. Our DFT calculations show that there are many molecular orbital in-plane transitions that contribute to this particular electronic transition, the most important being $4a'' \leftarrow 3a''$ (Table 3) which is essentially a $\pi^*_{C=O} \leftarrow \pi_{C=O}$ transition. We measured its oscillator strength as $f = 0.045$. We note that in formic acid, in the same spectral region (8–8.8 eV), there are very similar bands, with the same vibrational pattern and similar intervals, which we assigned to a valence π^*–π in-plane transition of oscillator strength $f = 0.2$ [32].The average band interval in the $5^1A' \leftarrow 1^1A'$ transition of acetic acid is 161 meV ($\approx$1300 cm^{-1}). This is close to five frequencies (mainly deformation) in ground state acetic acid, which are at 1181 (OH bend), 1280 (CCH_3 sym. deformation), 1380 (CCH_3 sym. deformation), 1434 (CCH_3 antisym. deformation)), and 1439 (CCH_3 antisym. deformation) cm^{-1} respectively [33]. The nature of the vibrational modes corresponds to the principal component of the potential energy distribution for each mode [33]. The successive frequency intervals are 1266, 1339, 1282 cm^{-1}, whereas in the PES first band they are 1500, 1470, 1450 cm^{-1} [31]. This casts doubt on the bands being part of a Rydberg series, although 3p is probably in this region (see later), (and indeed Robin assigns the C–X system to $3p \leftarrow n_O$ [28]). We remark that the profiles of these five vibronic bands could accommodate both valence and Rydberg components.

5) Higher energy valence transitions are calculated and must exist, no doubt intertwined with Rydberg transition bands. This is most probable in the 9–9.5 eV region, in which numerous sharp bands occur (Fig. 2), labeled by Bell et al. [9] as the D–X transition. However, of the many valence transitions calculated to lie at higher energies than $5^1A' \leftarrow 1^1A'$ (Table 3), only five are predicted by our DFT calculations to have appreciable oscillator strength, of which one, the $7^1A' \leftarrow 1^1A'(18a' \leftarrow 13a')$ transition we assign to band #25 at 9.732 eV. The other four valence transitions are expected to occur above 9.8 eV, in regions of high density of absorption features assigned to Rydberg transitions (Fig. 3). We recall that just as in the case of formic acid, where five valence transitions were analysed [32], there might occur valence-Rydberg mixing for some states of acetic acid.

4.2.3. Rydberg states and transitions of CH_3COOH

We will initially be concerned with two main classes of Rydberg transitions in acetic acid, those involving promotion of a 13a′ orbital electron leading at $n = \infty$ to the ion ground state $1^2A'$, and those where promotion of a 3a″ orbital electron leads eventually to the first excited state $1^2A''$ of the ion. Rydberg transitions involving higher energy ionization limits are discussed in Section 5.

There are various possible Rydberg series corresponding to transitions to non-degenerate s orbitals and to split core p and d orbitals. The Rydberg series transitions leading to the ground state of the ion are:

$$
\begin{aligned}
&n\text{sa}' \leftarrow 13\text{a}';\\
&n\text{pa}' \leftarrow 13\text{a}'; \quad n\text{pa}'' \leftarrow 13\text{a}'; \quad n\text{pa}' \leftarrow 13\text{a}'\\
&n\text{da}' \leftarrow 13\text{a}'; \quad n\text{da}'' \leftarrow 13\text{a}'; \quad n\text{da}' \leftarrow 13\text{a}';\\
&n\text{da}'' \leftarrow 13\text{a}'; \quad n\text{da}' \leftarrow 13\text{a}',
\end{aligned}
$$

the transitions being $^1A' \leftarrow 1^1A'$ when the Rydberg orbital has a′ symmetry, and $^1A'' \leftarrow 1^1A'$ when it has a″ symmetry.

Rydberg transitions that can lead to the first excited state of the ion are:

$$
\begin{aligned}
&n\text{sa}' \leftarrow 3\text{a}'';\\
&n\text{pa}' \leftarrow 3\text{a}''; \quad n\text{pa}'' \leftarrow 3\text{a}''; \quad n\text{pa}' \leftarrow 3\text{a}''\\
&n\text{da}' \leftarrow 3\text{a}''; \quad n\text{da}'' \leftarrow 3\text{a}''; \quad n\text{da}' \leftarrow 3\text{a}'';\\
&n\text{da}'' \leftarrow 3\text{a}''; \quad n\text{da}' \leftarrow 3\text{a}'',
\end{aligned}
$$

the transitions here being $^1A' \leftarrow 1^1A'$ when the Rydberg orbital has a″ symmetry, and $^1A'' \leftarrow 1^1A'$ when it has a′ symmetry.

The maximum oscillator strength for a Rydberg transition is found empirically to be $f = 0.08$ per spatial degeneracy [28]. A useful criterion is that transitions to $^1A''$ states should in general be much weaker than to $^1A'$ states.

The Rydberg series absorption bands should have upper states whose geometry is similar to that of the acetic acid ion state to which they converge at their limits. The electron configuration of the $1^2A'$ ground state of the ion leads us to conjecture that in the Rydberg series leading to this ion state, we should find progressions in vibrational modes similar to those observed in the first band of the photoelectron spectrum of acetic acid, and of similar relative intensities of the vibrational components. The HeI PES shows a principal progression in a mode of frequency ≈1480 cm^{-1} [31]. We therefore searched among the absorption bands in the expected Rydberg regions for sets of bands showing these interval characteristics (see below). This 1480 cm^{-1} frequency is most probably that of a CO stretch vibration, decreased from the 1788 cm^{-1} of the corresponding ν_4 mode in the ground state of neutral acetic acid. This decrease further confirms our assignment of the 4a″ molecular orbital to an antibonding $\pi^*_{C=O}$ LUMO. A weaker secondary progression in this mode at about 315 cm^{-1} from the origin band also occurs in the HeI PES first band [31].

In the $1^2A''$ excited state of the ion, removal of the 3a″ electron from the neutral ground state configuration should, following the analogous behaviour in formic acid [32], lead to an increase in the C=O bond length, a decrease in the C–O bond length and marked increases in the H′O′C and HCO′ angles, as well as a decrease in the OCO′ angle. The actual behaviour of the carbon–oxygen stretch vibrations in the HeI PES of formic acid and its isotopomers is more complex than these expectations [34,35].

4.3. Spectral assignments of Rydberg transitions below the ion ground state

The valence transitions were discussed in Section 4.2.2. We now discuss the Rydberg transition bands, beginning with those below the ion ground state energy.

4.3.1. ns ← 13a′ Rydberg series

The 3sa′ ← 13a′ Rydberg transition is expected to give rise to a broad diffuse feature, similar to the corresponding transition in formic acid. Robin [28] assigns a broad feature at 7.08 eV (cf. Fig. 2) as this Rydberg transition in acetic acid, which would give a value of $\delta = 1.04$ for the quantum defect of the 3s level; this is a reasonable value for a well-behaved s Rydberg orbital. Ari and Güven [11] assign an EELs feature at 7.1 eV to the 3sa′ ← 13a′ Rydberg transition, in agreement with Robin. As mentioned earlier, the 3sa′ ← 13a′ Rydberg transition could also occur in the region of the broad band whose maximum is at 7.795 eV (Fig. 2). If it were actually at 7.795 eV, this would correspond to a quantum defect $\delta = 0.80$, which is also quite possible for a 3s orbital exhibiting strong penetration [28].

We searched for higher members of the ns series. For $n = 4$ a suitable region to explore is 9–9.5 eV (Fig. 3). This contains 3 series of bands, α, β, γ, whose first members are respectively bands #9, 10, 11 (Table 1), and whose further members are separated by an interval of about 1490 cm^{-1}. This interval is similar to the vibrational frequency (≈1480 cm^{-1}) observed by PES in the ion ground state [31]. The vibrational mode is undoubtedly the C=O stretch vibration and we designate it as ν_4, following the acetic acid ground state vibration nomenclature of Bertie and Michaelian [36].

The α–β and β–γ intervals for corresponding members of the series are on average 372 cm^{-1}. This is most probably related to the weak progression of about 320–380 cm^{-1} observed in the first PES Band [31], as discussed later. The corresponding vibrational mode is the in-plane OCO bending vibration ν_{12}, which has a frequency of 439 cm^{-1} in the acetic acid ground state in the gas phase [36]. We considered in turn the first members of the α, β and γ series as potential 4s ← 13a′ Rydberg transitions. This gave quantum defect values $\delta = 1.103$ (a), 1.061 (b), 1.019 (c), all of which are compatible with $n = 4$, the differences being due the ion limit being considered as the vibrationless level in each case.

Following this up with searching for $n = 5$, we find at higher energies three series of bands, ε, ζ, η, with similar intervals to those found for the α, β, γ series, and whose first members are respectively bands #26, 27 and 28 (Table 1). The ε–ζ and ζ–η intervals for corresponding members of the series are on average 398 cm^{-1} and are assigned to the OCO bend vibration v_{12}. The assignments gave a quantum defect value $\delta = 0.96$ (ε), compatible with $n = 5$. The fact that the secondary intervals (about 380 cm^{-1}) are constant in going from $n = 4$ to 5 indicate that these intervals are linked to vibrations, or that different Rydberg l values are involved. As we will see later, the secondary intervals, observed for both ns and np Rydbergs, are, within experimental error, constant as a function of n, which argues in favour of vibrational components rather than different electronic series.

Similar series of bands were observed and assigned for $n = 6$ and 7 (Table 1). The search for $n = 8$ was infructuous. The increased density of features in this spectral region does not make it possible to choose secondary series with confidence.

4.3.2. The np ← 13a′ Rydberg series

The principal band of the two possible 3pa′ ← 13a′ Rydberg transitions, supposing $\delta = 0.6$, would be predicted to occur at about 8.253 eV. This is precisely in the region of the so-called C–X transition bands [9], which we have previously assigned to the valence transition, although, as mentioned earlier, Robin [28] assigns the C–X system to 3p ← n_O and we have remarked that the vibrational profiles could accommodate both valence and Rydberg components.

We now examine higher members of the np series using δ values of this order of magnitude.

The 4pa′ ← 13a′ Rydberg transition origin can be assigned to band #19, giving $\delta = 0.60$. The bands #19, 23, 26 form a series with an average interval of 1395 cm^{-1}, corresponding to vibrational mode v_4. In analogous fashion, the 5pa′ ← 13a′ Rydberg transition origin was assigned to band #29, giving $\delta = 0.57$. The bands #29, 33, 38 form a v_4 progression with an average interval of 1456 cm^{-1}. The origin band of the 6pa′ ← 13a′ Rydberg transition was found to be band #35, giving $\delta = 0.61$. The v_4 progression bands #35, 40, 45 have an average frequency interval of 1424 cm^{-1}. We were also able to assign the 7pa′ ← 13a′ Rydberg transition origin to band #38, giving $\delta = 0.60$. The bands #38, 44 form a v_4 progression with an average interval of 1420 cm^{-1}.

Secondary components of the np Rydberg series were less obvious than for the ns series. These components could be masked by being within the profiles of other bands, assigned otherwise. Higher spectral resolution and deuterium isotope studies are required to further the analysis.

In all, we have assigned $n$pa′ ← 13a′ Rydberg transitions, and their companion bands, for $n = 3$–7, and for which the quantum defects are essentially in the range 0.57–0.61 (Table 1). The possible np′a′ ← 13a′ Rydberg transitions were not assigned, but they are expected to be much weaker than the npa′ ← 13a′ Rydberg transitions.

4.3.3. The nda′ ← 13a′ Rydberg series

In formic acid the nd series has quantum defect values of the order of $\delta = 0.14$. For acetic acid, trial $\delta = 0.14$, gives 8.952 eV for $n = 3$. There is a weak band at 8.948 eV (#8), corresponding to $\delta = 0.143$. A series can be built up with band #8 as origin followed by bands #12, 16 and 21 as a v_4 progression, with an average interval 1444 cm^{-1}. We were also able to assign $n = 4$ and 5 transitions, with satisfactory quantum defect values respectively, 0.15 and 0.13 (Table 1).

Although for each value of n, there are expected three $n$da′ ← 13a′ transitions, it is probable that one of these transitions has the major oscillator strength. In any case, we do not observe more than one $n$da′ ← 13a′ transition for each value of n. We do not assign any low frequency companion bands. There are no previous reports of nd Rydberg series for acetic acid.

4.3.4. Vibrational frequencies of the Rydberg states converging to the ground state of the acetic acid ion

Two vibrational modes were excited in the Rydberg levels, giving rise to the companion bands discussed above. The average values of the frequencies over all companion bands in the ns, np and nd Rydberg series converging to the ground state of the ion are $v = 1463$ and 385 cm^{-1}. These values are very close to, and within the error limits of, the frequencies of the two principal ion ground state vibrations, $v = 1450$ (±30)–1500 (±20) cm^{-1} and $v = 310$ (±20)–380 (±20) cm^{-1} observed in photoelectron spectra [31].

As mentioned above, the frequencies $v = 1463$ and $v = 385$ cm^{-1} are assigned to C=O valence and OCO bend vibrations, whose neutral ground state frequencies are $v_4 = 1788$ cm^{-1} and $v_{12} = 439$ cm^{-1}, respectively. The large decrease in the v_4(C=O) frequency is similar to what is observed for formic acid, which has a similar HOMO to that of acetic acid, and in which the neutral v_4(C=O) = 1777 cm^{-1}, whereas the ground state ion v_4(C=O) = 1495 cm^{-1} [34].

4.4. Spectral assignments: Rydberg transitions converging to the first excited ion state $1^2A''$

Assignments of Rydberg bands converging to the first excited electronic state, $1^2A''$, of the acetic acid ion have not previously been reported. In searching for these Rydberg bands we started with the following two criteria:

1) We expect to find an energy interval ΔE of the order of 1.015 eV between the ns, np and nd Rydberg transition bands converging to the ground state of the ion and the corresponding series of bands which converge to the first excited state, since this is the value of the difference in the energies of these two ion states.

2) The existence of companion bands to the Rydberg transition O_0^0 origin band at intervals similar to those of vibrational frequencies of the first excited ion state.

4.4.1. n(s,p,d) ← 3a″ Rydberg series

The *n*sa′ ← 3a″ Rydberg series bands correspond to out-of-plane $^1A'' \leftarrow X^1A'$ transitions, so they are not expected to be very intense. The 3sa′ ← 3a″ origin band would be expected to be in the 8.7 eV region, and may be part of the background to the structure in this spectral region (Fig. 2). We assigned the origin band of the 4sa′ ← 3a″, band #34 ($\delta = 0.99$) and its ν_4 vibration companion band #39, as well as the 5sa′ ← 3a″, band #53 ($\delta = 0.89$) (Table 1). Because of the expected weakness of the *n*sa′ ← 3a″ transitions, we were unable to identify further members of this Rydberg series in the absorption spectrum.

For the *n*p ← 3a″ Rydberg series, on symmetry grounds one expects only one strong *n*p ← 3a″ transition, i.e. *n*pa″ ← 3a″. With assumed $\delta = 0.6$, the 3pa″ ← 3a″ transition origin band can be expected to occur at 9.268 eV, and this corresponds precisely to band #15 (Fig. 2), already assigned to 4sa′ ← 13a′($4_0^1 12_0^2$) vibronic transition. series above. The intensity and profile of this band is such that it is reasonable to consider that it also contains the 3pa″ ← 3a″ transition origin band. A ν_4 companion band (band #20) is also observed. Higher members of this Rydberg series are also assigned: 4pa″ ← 3a″ and 5pa″ ← 3a″ and their ν_4 companion bands (Table 1). Because of the high density of spectral lines in the 10–11.2 eV region (Fig. 3), higher spectral resolution and deuterium isotope studies would be useful to verify these assignments.

Band #36 was assigned to the 3d ← 3a″ Rydberg transition, with a $\delta = 0.06$. Higher members of this series assigned are band #50 (4d,$\delta = 0.12$), and band #56, as the the 5d ← 3a″ ($\delta = 0.17$) Rydberg transition (Table 1).

The average value of the ν_4 vibrational mode frequency in these Rydberg progressions to the $2^2A''$ ion state is 1521 cm^{-1}. This is smaller than the neutral ground state frequency, as expected from the bonding characteristics of the molecular orbitals, but is somewhat higher than the average value, 1463 cm^{-1}, for the ν_4 mode in Rydbergs converging to the ion ground state. This behaviour is similar to the case of the corresponding Rydberg and ion limit states of formic acid [32]. Knowledge of vibrational frequencies in the $2^2A''$ ion state from photoelectron spectroscopy is scarce. Values for two frequencies are given by Watanabe et al. from PES measurements [31], but the vibrational components of the photoelectron second band are very poorly resolved, so that these frequencies are not known with any reliable accuracy. Watanabe et al. consider that the vibrational structure of the second PES band is similar to that of the corresponding band of formic acid but this remains to be confirmed.

5. Absorption at higher energies: 12–20 eV

The absorption spectrum above the second ionization energy can be seen in Fig. 1. There are no previous reports concerning absorption spectra of acetic acid in the 11.7–20 eV region but there are published EELS spectra, up to 15.5 eV [11], whose energy resolution is very much less than that of our absorption spectra. The EELs spectrum shows a broad continuous feature between 12 and 15.5 eV, peaking in the 13 eV region. Our absorption spectrum shows several broad features between 12 and 20 eV (Fig. 1). Twin, hardly resolved, absorption features occur at 12.92 eV (53.6 Mb) and 13.33 eV (53.3 Mb), which doubtless correspond to the EELS peak at 13 eV. The minimum at 13.75 eV is followed by a stronger peak at 14.5 eV (60.2 Mb), not detected in the EELS spectrum, followed by a minimum at 14.9 eV after which the absorption curve rises to a maximum of 72.2 Mb at 16.83 eV, with two inflexions at 15.125 and 15.77 eV.

In order to analyse the absorption spectra observed between 12 and 20 eV region we first discuss the ion states in this region, which should be the limit states to which Rydberg series in this spectral region converge. Photoelectron spectroscopy has established a series of ion states arising by successive loss of an electron from molecular orbitals of CH_3COOH. In the 12–20 eV region there are ionization limits corresponding to loss respectively of the 2a″, 12a′, 11a′, 1a″, 10a′, 9a′ and 8a′ electrons in one electron transitions (Table 2). Loss of the 7a′ electron takes place at an energy about 4.1 eV above that of the 8a′ electron (Table 2), which is in the 20.3 eV region. We neglect any satellite states corresponding to two-electron transitions and configurational effects in general, which is reasonable for CH_3COOH below 20 eV, which we can expect to be similar to the case of HCOOH [37].

In Fig. 1 we give the absorption spectrum between 12.2 and 20 eV and have indicated the various vertical ionization limits. In this spectral region there are no notable features that can be directly linked to Rydberg transitions, nor do the band profiles appear to characterise Rydberg transition convergence to the various ion states, apart possibly from those corresponding to loss of the 2a″ and 11a′ electrons.

In this spectral region one can expect also π–σ*, σ–π* and σ–σ* transitions [38]. Assignment is hazardous, not only because of the complexity of the molecular orbitals relevant to this energy region, but also because the broadness of the VUV absorption features makes it difficult to determine the experimental transition energies. However, there exist some useful considerations. Two types of unoccupied σ* orbitals involving C–H groups have been discussed [39]. Excitation to these orbitals would correspond to high energy valence transitions. In type 1, the orbital is antibonding between carbon and hydrogen atoms ; in type 2 it is non-bonding and has little density on hydrogen atoms. The latter has been designated as n.h. (‘‘negligible hydrogen’’) orbitals by Lindholm et al. [39]. In the case

of the occupied orbitals, strong orbital mixing makes their separation into n.h. and non-n.h. impractical. From the discussion by Lindholm et al., in particular on formic acid, one can predict that in acetic acid strong σ–σ* (C–H) and σ–σ* (C–C) n.h. transitions should occur in the 12–18 eV region, with the latter being at higher energy than the σ–σ* (C–H) non-n.h. transition.

We propose that the #59 and #60 features correspond to broad overlapping Rydberg bands converging to the $2^2A''$ ($-2a''$) ion state, that band #61 corresponds to a valence σ–σ* (C–H) non-n.h. transition, while band #64 is the σ–σ* (C–H) transition. Features #62 and #63 may correspond to overlapping Rydberg bands converging to still higher ion state limits. Collective π electron excitation can also be expected in the 16–20 eV region [38] and probably contributes to the broad background absorption in this spectral region. It is of interest that the peak absorbance of acetic acid, 72.2 Mb, which occurs at 16.9 eV, is of the same order of magnitude of that of other species containing 8 atoms, e.g. C_2H_6 (80 Mb) [40].

6. Conclusion

Absorption spectra of CH_3COOH were measured between 6 and 20 eV. In our analysis of the spectra we discuss and use the molecular orbital structure of acetic acid, the associated bonding properties, and our theoretical calculations on valence states of this acid. Data on ionic states and their structural and dynamic properties, obtained from He I photoelectron spectroscopy of acetic acid [20,21,25,26,31] were also used. Valence transitions and the different types of expected Rydberg transitions converging to the ground state $1^2A'$ and the first excited electronic state $1^2A''$ of the formic acid ion were first discussed. The corresponding valence and Rydberg absorption bands were then assigned in the spectral region below 11.2 eV. Earlier studies have been limited to an upper energy limit of 11.7 eV. In the spectral region common to previous measurements, we observed and assigned many features seen by previous authors [28], in particular by Bell et al. [9]. This has involved re-assignment, or assignment for the first time of reported absorption spectral features. Previous to our study, there was no concerted identification and analysis of Rydberg transitions of acetic acid, apart from suggestions concerning 3s and 3p levels of Rydbergs converging to the ion ground state. Our analysis identifies ns, np and nd transitions. Two vibrational companions to the Rydberg series converging to the ion ground state were observed, corresponding to excitation of the C=O stretch vibration ν_4 and the OCO bend vibration ν_{12}. Because of spectral congestion it was more difficult to identify Rydberg bands converging to the first excited ion state, but we succeeded in assigning ns, np and nd Rydberg transitions in which the $3a''$ electron is excited. Higher spectral resolution and deuterium isotopic studies would be useful in for confirming and extending the Rydberg analysis.

Entirely novel aspects of our study concern the observation, analysis and assignment of absorption features at higher energies, between 12 and 20 eV, observed and carried out here for the first time. The existence of Rydberg bands was explored for transitions whose limiting ion states are respectively $2^2A''$, $2^2A'$, $3^2A'$, $3^2A''$, $4^2A'$, $5^2A'$ and $6^2A'$, corresponding to ionization of electrons from the successive molecular orbitals $2a''$, $12a'$, $11a'$, $1a''$, $10a'$, 9a and $8a'$. Rydberg bands converging to these ionization limits were not observed as distinct discrete features. The Rydberg bands converging to the other ionization limits are apparently broad and merge to form the broad features or underlying continuous absorption observed in specified high energy regions. Broad bands in the 14 – 17 eV region suggested assignments in terms of two types of σ–σ valence transitions, probably also involving collective π electron excitation.

The detailed information obtained in the present absorption study is of direct use not only in the interpretation of acetic acid dissociative photoionization but also for other photophysical properties, such as fluorescence emission observed from neutral and ionic dissociation channels as a function of excitation energy [8]. As mentioned in Section 1, this information is of direct interest for interpreting certain observations of atmospheric and astrophysical phenomena, for predicting regions of the interstellar medium liable to contain acetic acid, and for general exobiology studies in which acetic acid plays a role as a building block of biomolecules.

Acknowledgements

We acknowledge the Centre de Calcul Recherche et Technologie, CEA Saclay, for computing resources and the use of the Gaussian-03 program. The experiments were carried out at the BESSY I synchrotron facility in Berlin, supported by the TMR programme of the European Union under contract FMRX-CT-0126. Support from the CNRS Groupe de Recherche "GDR Exobiologie" (GDR 1877) is gratefully acknowledged.

References

[1] D.K. Harvey, K.J. Feieraband, J.C. Black, V. Vaida, J. Molec. Spectrosc. 229 (2005) 151.
[2] A. Brack (Ed.), The Molecular Origins of Life, Cambridge University Press, Cambridge, UK, 1998.
[3] S.L. Miller, in [2], pp. 59–85.
[4] D.H. Mehringer, L.E. Snyder, Y. Miao, F.J. Lovas, Ap. J. 480 (1997) L71.
[5] W.M. Irvine, P. Friberg, N. Kaifu, H.E. Mathews, Y.C. Minh, M. Ohishi, S. Ishikawa, Astron. Astrophys. 229 (1990) L9.
[6] Y.-J. Kuan, S.B. Charnley, H.-C. Huang, W.L. Tseng, Z. Kisiel, Astrophys. J. 593 (2003) 848.
[7] J. Crovisier, D. Bockelée-Morvan, P. Colom, N. Biver, D. Despois, D.C. Lis, Astron. Astrophys. 418 (2004) 1141.
[8] S. Leach, M. Schwell, H.-W. Jochims, H. Baumgärtel, Chem. Phys., 2005, this issue, doi:10.1016/j.chemphys.2005.08.020.
[9] S. Bell, T.L. Ng, A.D. Walsh, J. Chem. Soc. Faraday Trans. II 71 (1975) 393.

[10] M. Suto, X. Wang, L.C. Lee, J. Phys. Chem. 92 (1988) 3764.
[11] T. Ari, H.H. Güven, J. Electron Spectrosc. Rel. Phen. 106 (2000) 29.
[12] E.E. Barnes, W.T. Simpson, J. Chem. Phys. 39 (1963) 670.
[13] S. Nagakura, K. Kaya, H. Tsubomura, J. Molec. Spectrosc. 13 (1964) 1.
[14] A. Hoxha, R. Locht, B. Leyh, D. Dehareng, K. Hottmann, H.W. Jochims, H. Baumgärtel, Chem. Phys. 260 (2000) 237.
[15] M.J. Frisch, G.W. Trucks, H.B. Schlegel, G.E. Scuseria, M.A. Robb, J.R. Cheeseman, J.A. Montgomery Jr., T. Vreven, K.N. Kudin, J.C. Burant, J.M. Millam, S.S. Iyengar, J. Tomasi, V. Barone, B. Mennucci, M. Cossi, G. Scalmani, N. Rega, G.A. Petersson, H. Nakatsuji, M. Hada, M. Ehara, K. Toyota, R. Fukuda, J. Hasegawa, M. Ishida, T. Nakajima, Y. Honda, O. Kitao, H. Nakai, M. Klene, X. Li, J.E. Knox, H.P. Hratchian, J.B. Cross, C. Adamo, J. Jaramillo, R. Gomperts, R.E. Stratmann, O. Yazyev, A.J. Austin, R. Cammi, C. Pomelli, J.W. Ochterski, P.Y. Ayala, K. Morokuma, G.A. Voth, P. Salvador, J.J. Dannenberg, V.G. Zakrzewski, S. Dapprich, A.D. Daniels, M.C. Strain, O. Farkas, D.K. Malick, A.D. Rabuck, K. Raghavachari, J.B. Foresman, J.V. Ortiz, Q. Cui, A.G. Baboul, S. Clifford, J. Cioslowski, B.B. Stefanov, G. Liu, A. Liashenko, P. Piskorz, I. Komaromi, R.L. Martin, D.J. Fox, T. Keith, M.A. Al-Laham, C.Y. Peng, A. Nanayakkara, M. Challacombe, P.M.W. Gill, B. Johnson, W. Chen, M.W. Wong, C. Gonzalez, J.A. Pople, GAUSSIAN-03, Revision B.05, Gaussian Inc., Pittsburgh, PA, 2003.
[16] J.L. Derissen, J. Molec. Struct. 7 (1971) 67.
[17] R.E. Stratmann, G.E. Scuseria, M.J. Frisch, J. Chem. Phys. 109 (1998) 8218.
[18] G. Schaftenaar, J.H. Noordik, J. Comput.-Aided Mol. Design 14 (2000) 123.
[19] L. Turi, J.J. Dannenberg, J. Phys. Chem. 97 (1993) 12197.
[20] F. Carnovale, T.H. Gan, J.B. Peel, J. Electron Spectrosc. Rel. Phen. 20 (1980) 53.
[21] W. von Niessen, G. Bieri, L. Åsbrink, J. Electron Spectrosc. Rel. Phen. 21 (1980) 175.
[22] M.B. Robin, I. Ishii, R. McLaren, A.P. Hitchcock, J. Electron Spectrosc. Rel. Phen. 47 (1988) 53.
[23] S.G. Urquhart, H. Ade, J. Phys. Chem. B 106 (2002) 8531.
[24] N. Kosugi, H. Kuroda, Chem. Phys. Lett. 74 (1980) 490.
[25] P.H. Cannington, N.S. Ham, J. Electron Spectrosc. Rel. Phen. 31 (1983) 175.
[26] K. Kimura, S. Katsumata, T. Yamazaki, H. Wakabashi, J. Electron Spectrosc. Rel. Phen. 6 (1975) 41.
[27] H. Basch, M.B. Robin, N.A. Kuebler, J. Chem. Phys. 49 (1968) 5007.
[28] M.B. Robin, Higher Excited States of Polyatomic Molecules, I, II, III, Academic Press, Inc., London, 1974, 1975, 1985.
[29] D.J. Knowles, A.J.C. Nicholson, J. Chem. Phys. 60 (1974) 1180.
[30] Ya.Ya. Villem, M.E. Akopyan, Russ. J. Phys. Chem. 50 (1976) 394.
[31] I. Watanabe, Y. Yokoyama, S. Ikeda, Bull. Chem. Soc. Jpn 47 (1974) 627.
[32] S. Leach, M. Schwell, F. Dulieu, J.-L. Chotin, H.W. Jochims, H. Baumgärtel, Phys. Chem. Chem. Phys. 4 (2002) 5025.
[33] R.W. Williams, A.H. Lowrey, J. Comput. Chem. 12 (1991) 761.
[34] S. Leach, M. Schwell, D. Talbi, G. Berthier, K. Hottmann, H.W. Jochims, H. Baumgärtel, Chem. Phys. 286 (2003) 15.
[35] E. Rudberg, T. Brinck, Chem. Phys. 302 (2004) 217.
[36] J.E. Bertie, K.H. Michaelian, J. Chem. Phys. 77 (1982) 5267.
[37] J. Schirmer, L.S. Cederbaum, W. Domke, W. von Niessen, Chem. Phys. Lett. 157 (1978) 582.
[38] H.-W. Jochims, E. Rühl, H. Baumgärtel, S. Tobita, S. Leach, Int. J. Mass Spectrom. Ion Processes 167/168 (1997) 35.
[39] E. Lindholm, L. Åsbrink, S. Ljunggren, J. Phys. Chem. 95 (1991) 3923.
[40] J. Berkowitz, Photoabsorption, Photoionization and Photoelectron Spectroscopy, Academic, New York, 1979.